MR/Case Study

MSK Imaging using Advanced intelligent Clear-IQ Engine (AiCE) Deep Learning Reconstruction

Hung P. Do, PhD
Manager Medical Affairs – Sr. Clinical Scientist
Canon Medical Systems USA, Inc.

Dawn Berkeley
Manager Medical Affairs – Sr. Clinical Development
Canon Medical Systems USA, Inc.

Introduction

Magnetic Resonance Imaging (MRI) is routinely used for the diagnosis and treatment follow-up of musculoskeletal (MSK) disorders due to its ability to noninvasively image MSK tissues with the multiplanar view, high resolution, and excellent soft-tissue contrast. For MSK imaging, high resolution and high signal-to-noise (SNR) are desired for accurate diagnosis. However, higher SNR and resolution often require longer scan times due to fundamental tradeoffs between scan time, resolution, and SNR in MRI.

Advanced intelligent Clear-IQ Engine (AiCE) is the world's first fully integrated Deep Learning-based Reconstruction (DLR) introduced by major MRI manufacturers. Specifically, AiCE DLR is designed to remove Gaussian noise, hence, improving the SNR* of the MR images. Through the denoising process, image quality and SNR gain could assist clinicians in providing flexibility in scan parameters and be used to improve resolution and/or shorten scan time.

The case study report contains images collected from four clinical patients (two knees, one shoulder, and one hip) who underwent routine clinical MRI examinations using a 3T Vantage Galan scanner (Canon Medical Systems Corporation, Tochigi, Japan). In addition to routine clinical protocol, AiCE DLR-optimized protocol was performed. The cases are organized as follows:

- Case #1: Knee MRI with AiCE DLR
- Case #2: Knee MRI with AiCE DLR
- Case #3: Shoulder MRI with AiCE DLR
- Case #4: Hip MRI with AiCE DLR

* AiCE provides higher SNR compared to typical low pass filters.

Case #1: Knee MRI with AiCE DLR

MRI of the Right Knee—34-year-old male.

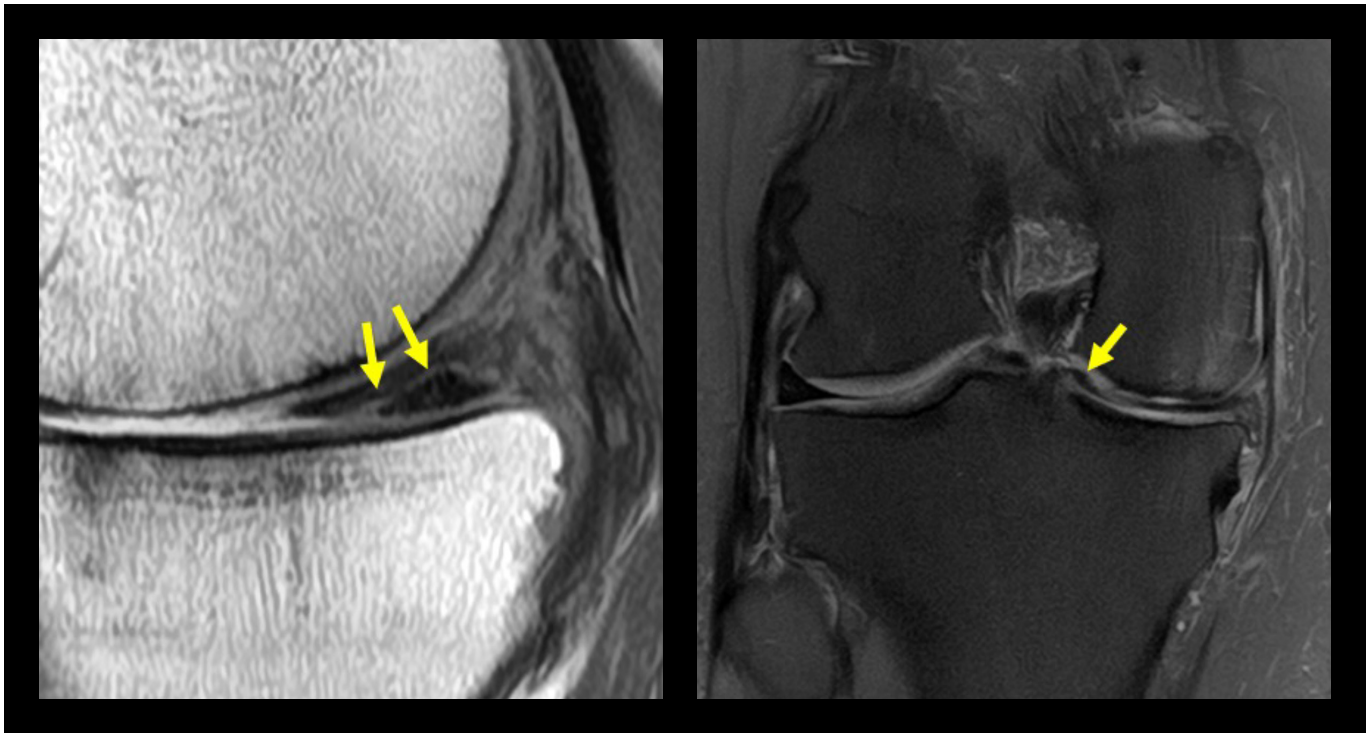

Figure 1.1: AiCE DL reconstructed zoom-in SAG PD (left) and COR PD FatSat (right). Horizontal oblique longitudinal tear (double yellow arrow) and flap (single yellow arrow) tear of medial meniscus body and posterior meniscal horn.

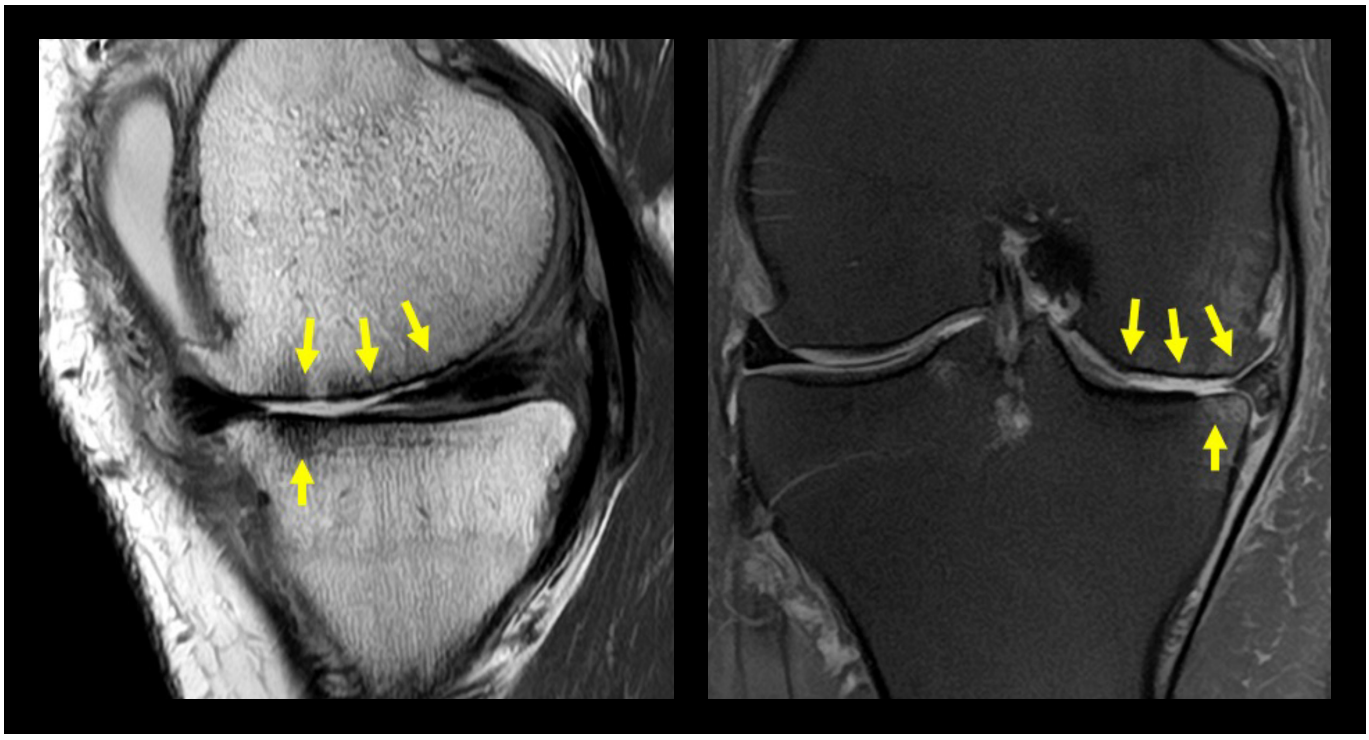

Figure 1.2: AiCE DL reconstructed SAG PD (left) and COR PD FatSat (right). Arrows show grade 4 severe chondral thinning to the bone of the medial tibial plateau and femoral condyle, demonstrating subchondral bone edema, flattening, and medial displacement extrusion of the medial meniscus.

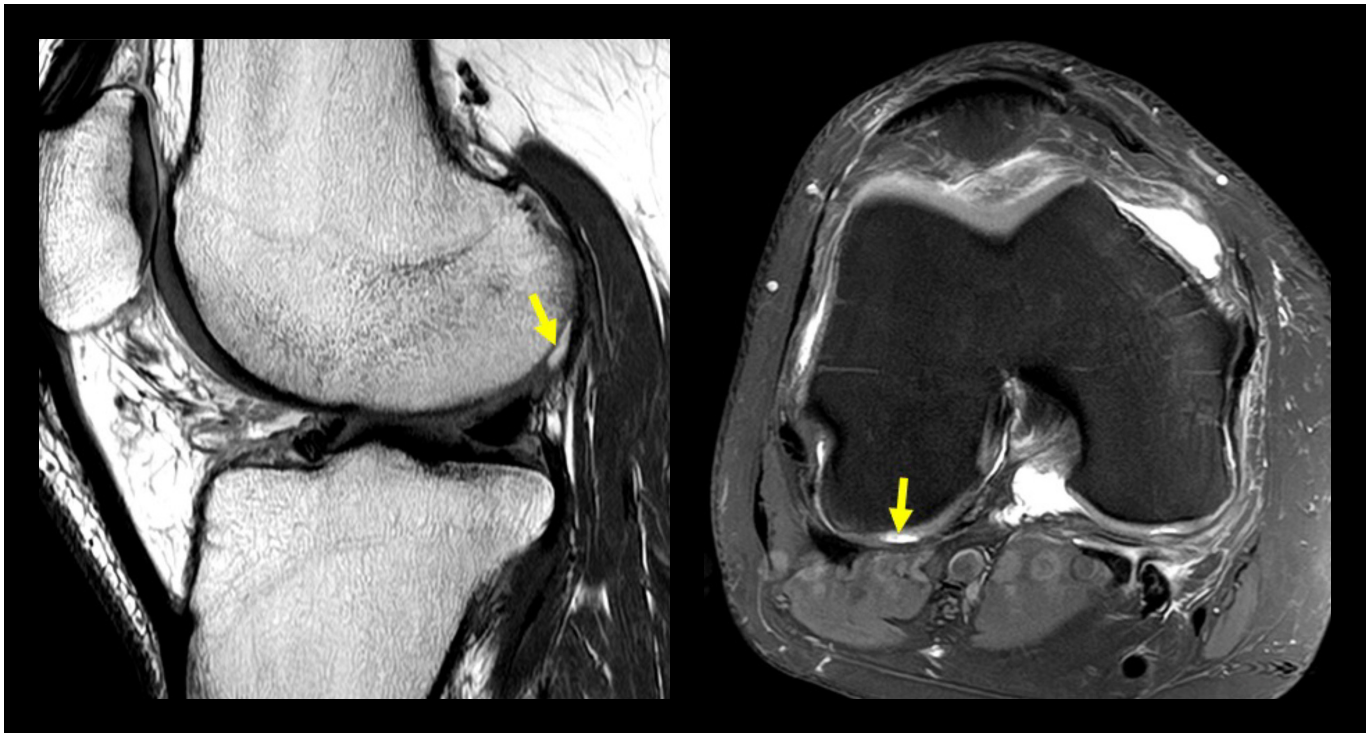

Figure 1.3: AiCE DL reconstructed SAG PD (left) and AX PD FatSat (right). Arrows show focal chondral defect posterior superior lateral femoral condyle.

Figure 1.4: AiCE DL reconstructed SAG PD. Blue arrow shows anterior fat pad and synovial notch scarring. Yellow arrow shows cyclops lesion or localized anterior arthrofibrosis along anterior notch and distal anterior cruciate ligament following arthroscopy.

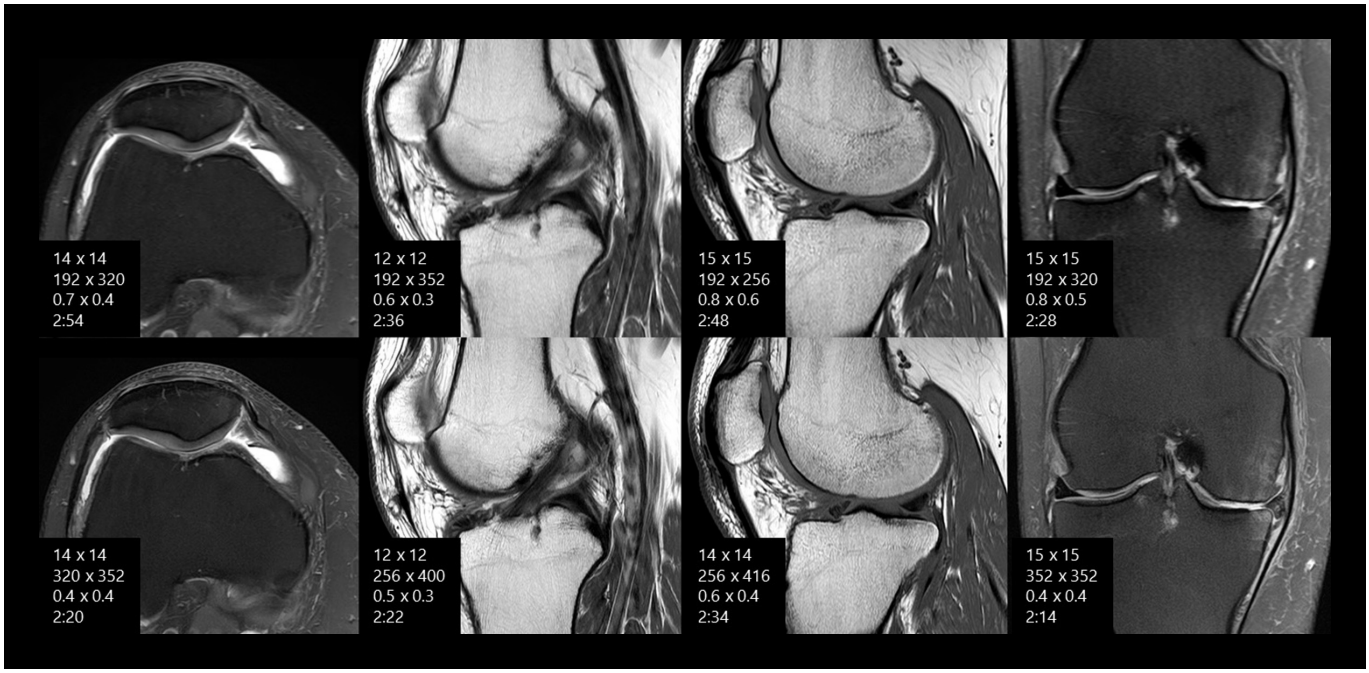

Figure 1.5: Routine images (top row) compared to the AiCE DLR-optimized images (bottom row) with higher resolution and/or shortened scan time.*

Case 1: Knee MRI with AiCE DLR								
	AX PD FatSat		SAG PD		SAG T1		COR PD FatSat	
	Routine	AiCE DLR	Routine	AiCE DLR	Routine	AiCE DLR	Routine	AiCE DLR
FOV	14 x 14	14 x 14	12 x 12	12 x 12	15 x 15	15 x 15	15 x 15	15 x 15
Matrix	192 x 320	320 x 352	192 x 352	256 x 400	192 x 256	256 x 416	192 x 320	352 x 352
Resolution (mm^2)	0.73 x 0.44 (0.32)	0.44 x 0.40 (0.17)	0.63 x 0.34 (0.21)	0.47 x 0.30 (0.14)	0.78 x 0.59 (0.46)	0.59 x 0.36 (0.21)	0.78 x 0.47 (0.37)	0.43 x 0.43 (0.18)
% Resolution Improvement*		**45.45%**		**34.00%**		**53.85%**		**50.41%**
Scan Time (Seconds)	2:54 (174)	2:20 (140)	2:36 (156)	2:22 (142)	2:48 (168)	2:34 (154)	2:28 (148)	2:14 (134)
% Scan Time Reduction*		**19.54%**		**8.97%**		**8.33%**		**9.50%**

	Routine	AiCE DLR
Total Scan Time (Seconds)	10:46 (646)	9:30 (570)
% Total Scan Time Reduction*		**11.76%**

	Routine	AiCE DLR
Average Resolution (mm^2)	0.73 x 0.46 (0.33)	0.48 x 0.37 (0.18)
% Average Resolution Improvement*		**46.74%**

Table 1: Sequence parameters of the routine protocol and the AiCE DLR-optimized protocol.

* Resolution and scan times vary by case. AiCE DLR-optimized protocol scan times and resolution are determined by the operator.

Case #2: Knee MRI with AiCE DLR

MRI of the Right Knee—24-year-old male.

Figure 2.1: AiCE DL reconstructed SAG PD FatSat (left) and COR PD FatSat (right) demonstrate a complete tear at the mid to proximal anterior cruciate ligament (ACL). Open arrow shows the tear defect. Solid arrows on the SAG view demonstrate proximal and distal remnants of torn ACL with posterior bowing. Solid arrow on the COR view indicates an ACL tear defect.

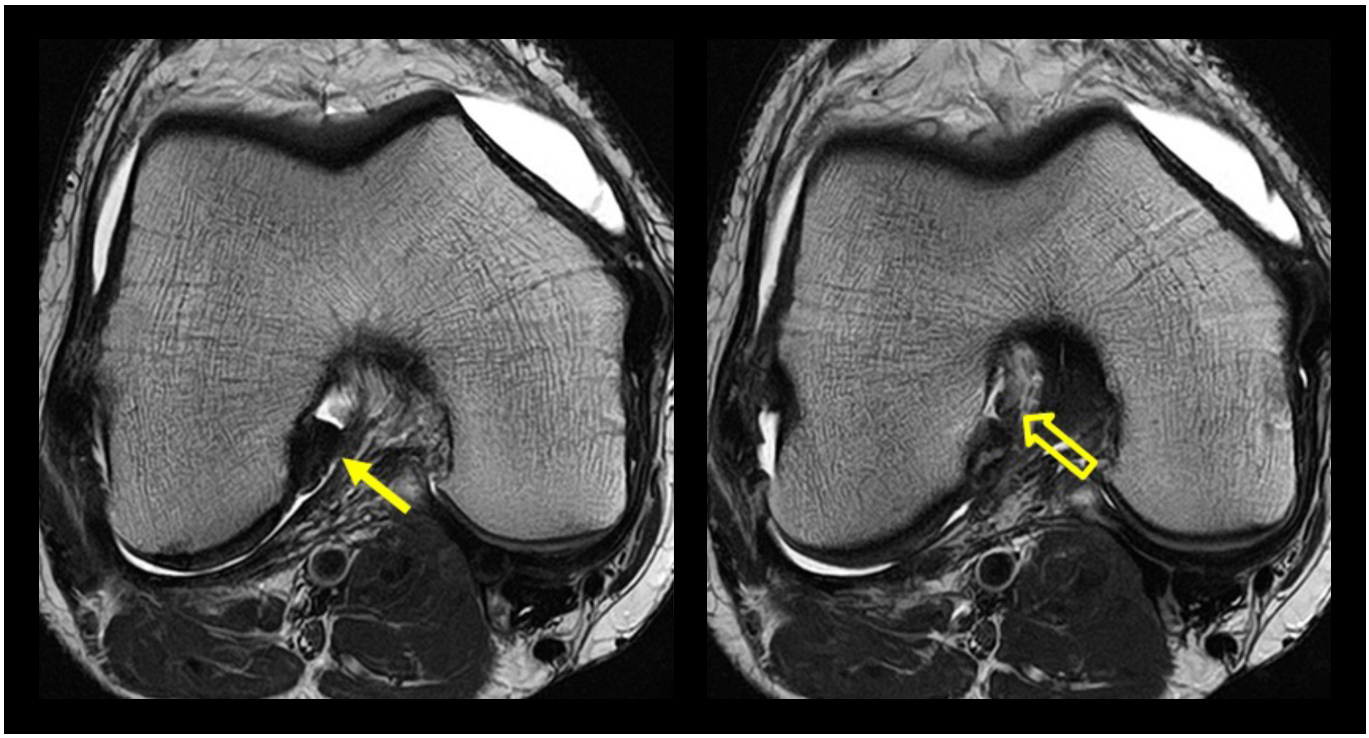

Figure 2.2: AiCE DL reconstructed AX T2 weighted images. Open arrow points to the ACL tear defect and solid arrow indicates the proximal remnant of ACL.

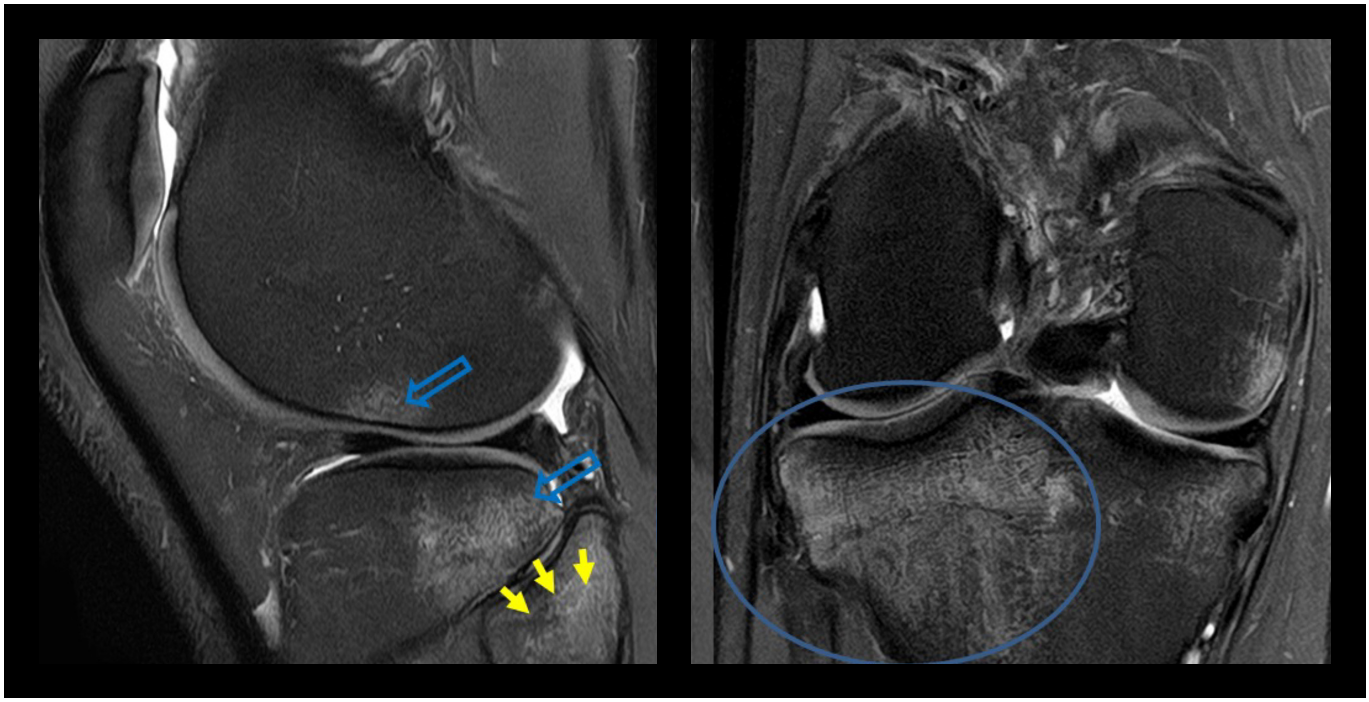

Figure 2.3: AiCE DL reconstructed SAG PD FatSat (left) and COR PD FatSat (right). Laterally, there is an impaction pattern typically associated with an acute ACL tear. This contusion pattern often results from a pivot-shift type injury common in skiers or football players. Blue circle indicates bone edema, contusion, and impaction of lateral tibial plateau. Open blue arrows indicate bone edema, contusion, and impaction of the lateral femoral condyle and tibial plateau. Solid yellow arrows show bone edema and contusion of the fibular head.

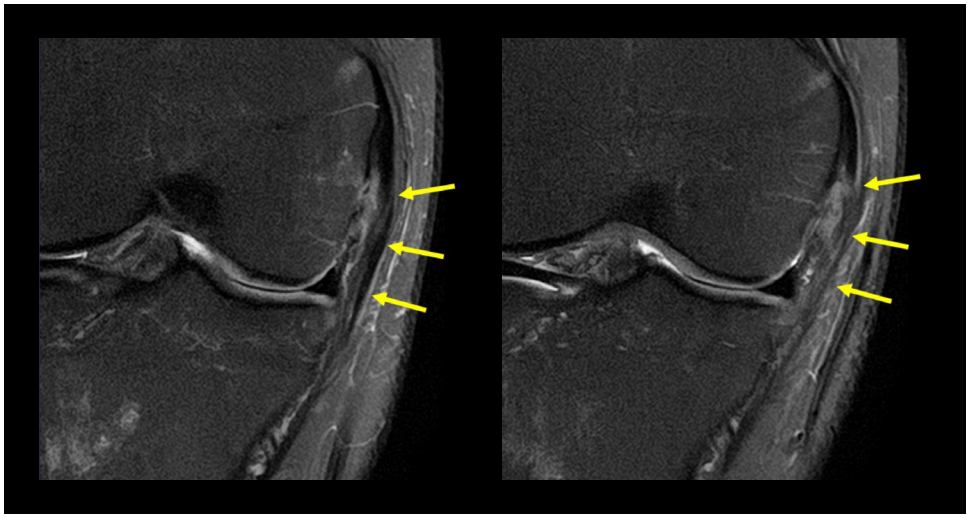

Figure 2.4: AiCE DL reconstructed COR PD FatSat images. Solid arrows indicate sprain and partial tear of proximal medial collateral ligament MCL.

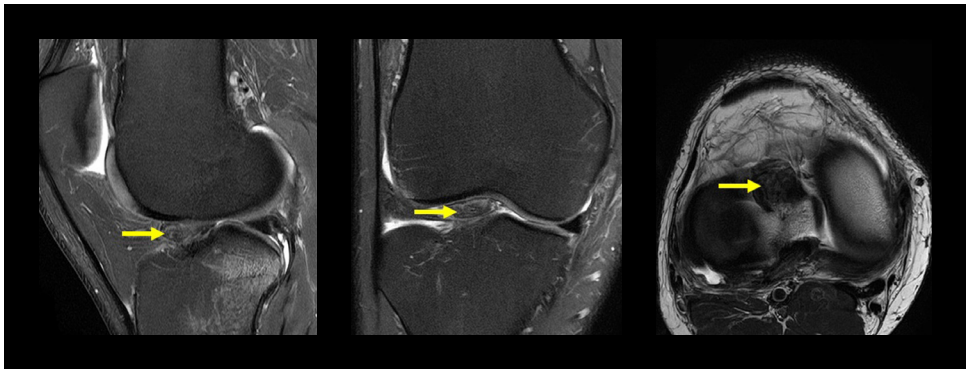

Figure 2.5: AiCE DL reconstructed SAG PD FatSat (left), COR PD FatSat (right), and AX T2 weighted images. Yellow arrows indicate scar mass in the anterior notch (intercondylar fossa).

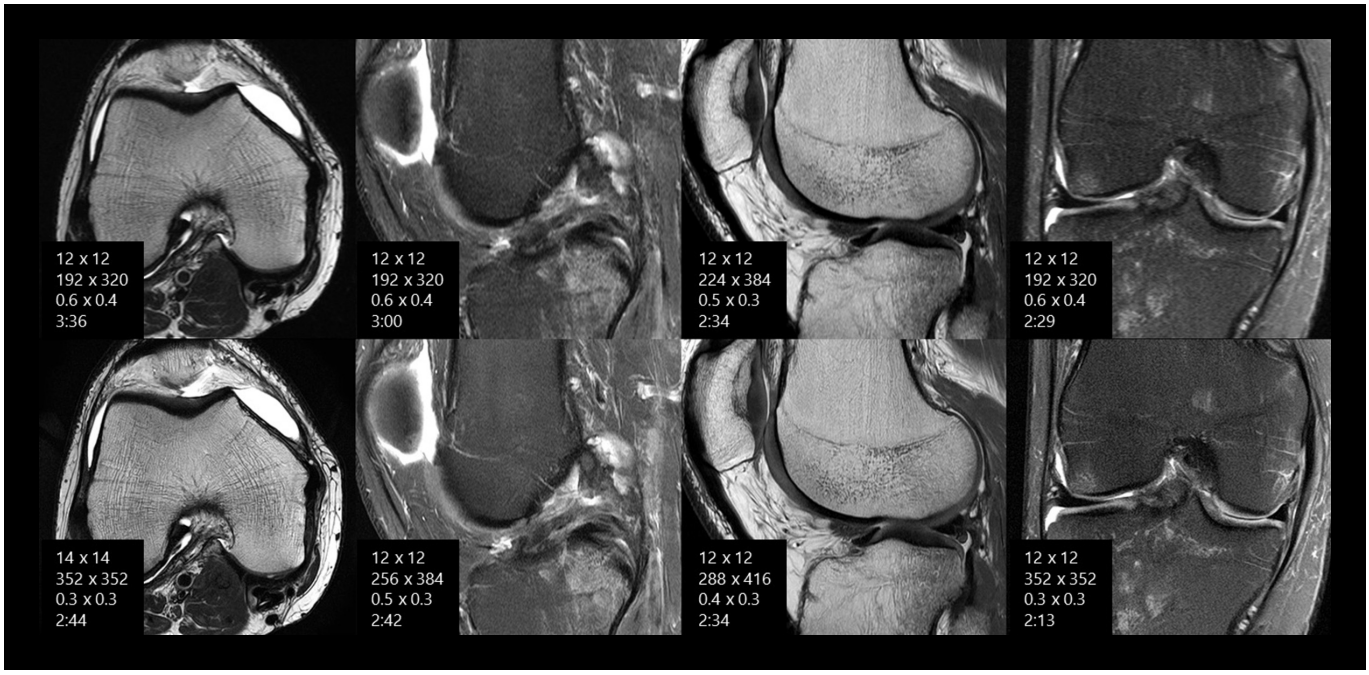

Figure 2.6: Routine images (top row) compared to the AiCE DLR-optimized images (bottom row) with higher resolution and/or shortened scan time.*

Case 2: Knee MRI with AiCE DLR								
	AX PD T2		SAG PD FatSat		SAG PD		COR PD FatSat	
	Routine	**AiCE DLR**	**Routine**	**AiCE DLR**	**Routine**	**AiCE DLR**	**Routine**	**AiCE DLR**
FOV	12 x 12	12 x 12	12 x 12	12 x 12	12 x 12	12 x 12	12 x 12	12 x 12
Matrix	192 x 320	352 x 352	192 x 320	256 x 384	224 x 384	288 x 416	192 x 320	352 x 352
Resolution (mm^2)	0.63 x 0.38 (0.23)	0.34 x 0.34 (0.12)	0.63 x 0.38 (0.23)	0.47 x 0.31 (0.15)	0.54 x 0.31 (0.17)	0.42 x 0.29 (0.12)	0.63 x 0.38 (0.23)	0.34 x 0.34 (0.12)
% Resolution Improvement*		**50.41%**		**37.50%**		**28.21%**		**50.41%**
Scan Time (Seconds)	3:36 (216)	2:44 (166)	3:00 (180)	2:42 (162)	2:34 (154)	2:34 (154)	2:29 (149)	2:13 (133)
% Scan Time Reduction*		**24.07%**		**10.00%**		**0%**		**10.74%**

	Routine	**AiCE DLR**
Total Scan Time (Seconds)	11:39 (699)	10:13 (613)
% Total Scan Time Reduction*		**12.30%**

	Routine	**AiCE DLR**
Average Resolution (mm^2)	0.60 x 0.36 (0.22)	0.39 x 0.32 (0.13)
% Average Resolution Improvement*		**41.99%**

Table 2: Sequence parameters of the routine protocol and the AiCE DLR-optimized protocol.

* Resolution and scan times vary by case. AiCE DLR-optimized protocol scan times and resolution are determined by the operator.

Case #3: Shoulder MRI with AiCE DLR

MRI of the Left Shoulder—77-year-old male.

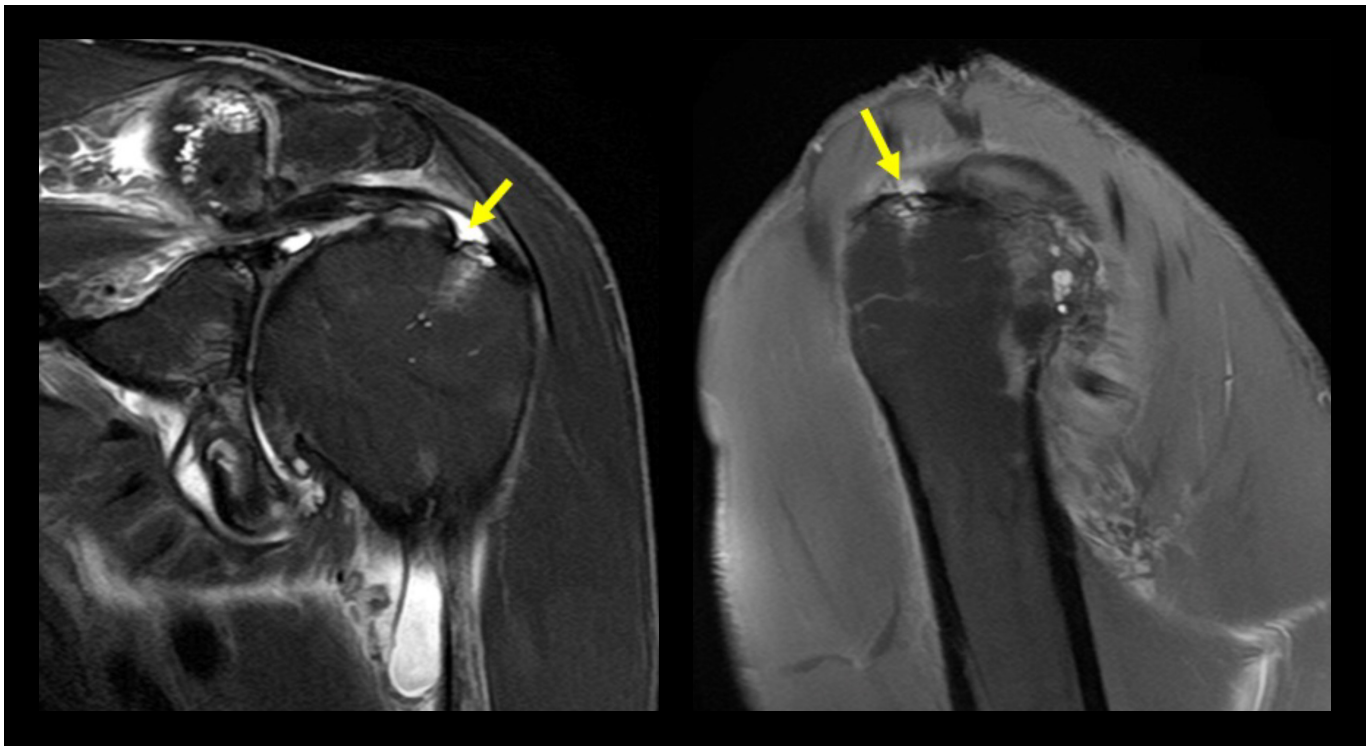

Figure 3.1: AiCE DL reconstructed COR T2 FatSat (left) and SAG PD FatSat (right). Arrows show rotator cuff tendinosis with oblique longitudinal tear and delamination of the distal anterior supraspinatus tendon.

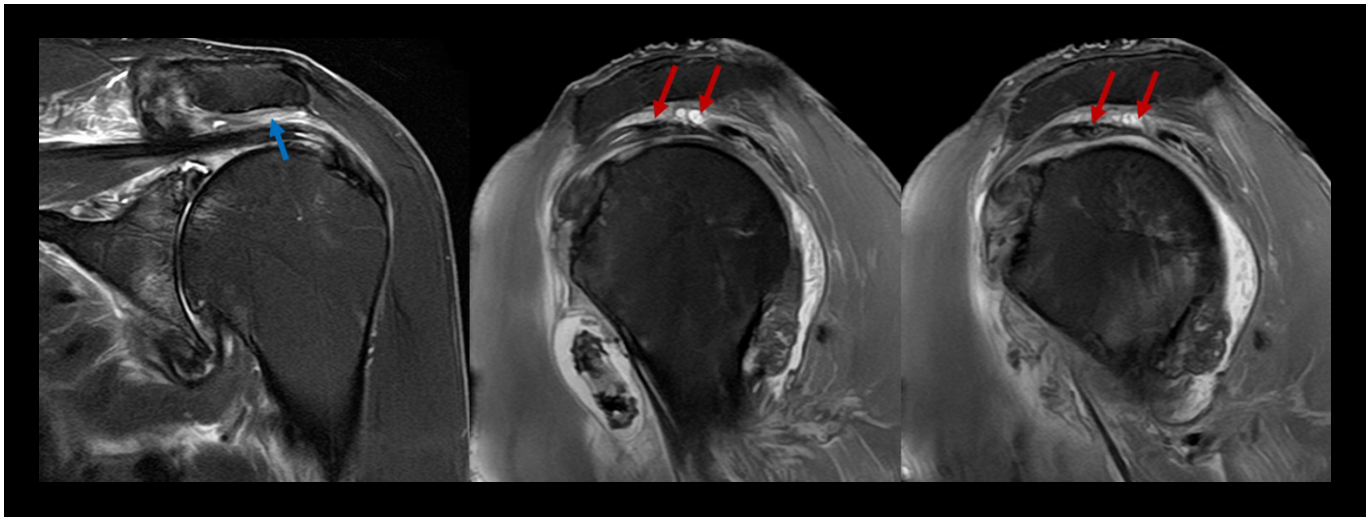

Figure 3.2: AiCE DL reconstructed COR T2 FatSat (left) and SAG PD FatSat (middle and right). Arrows show subacromial subdeltoid bursitis and scarring.

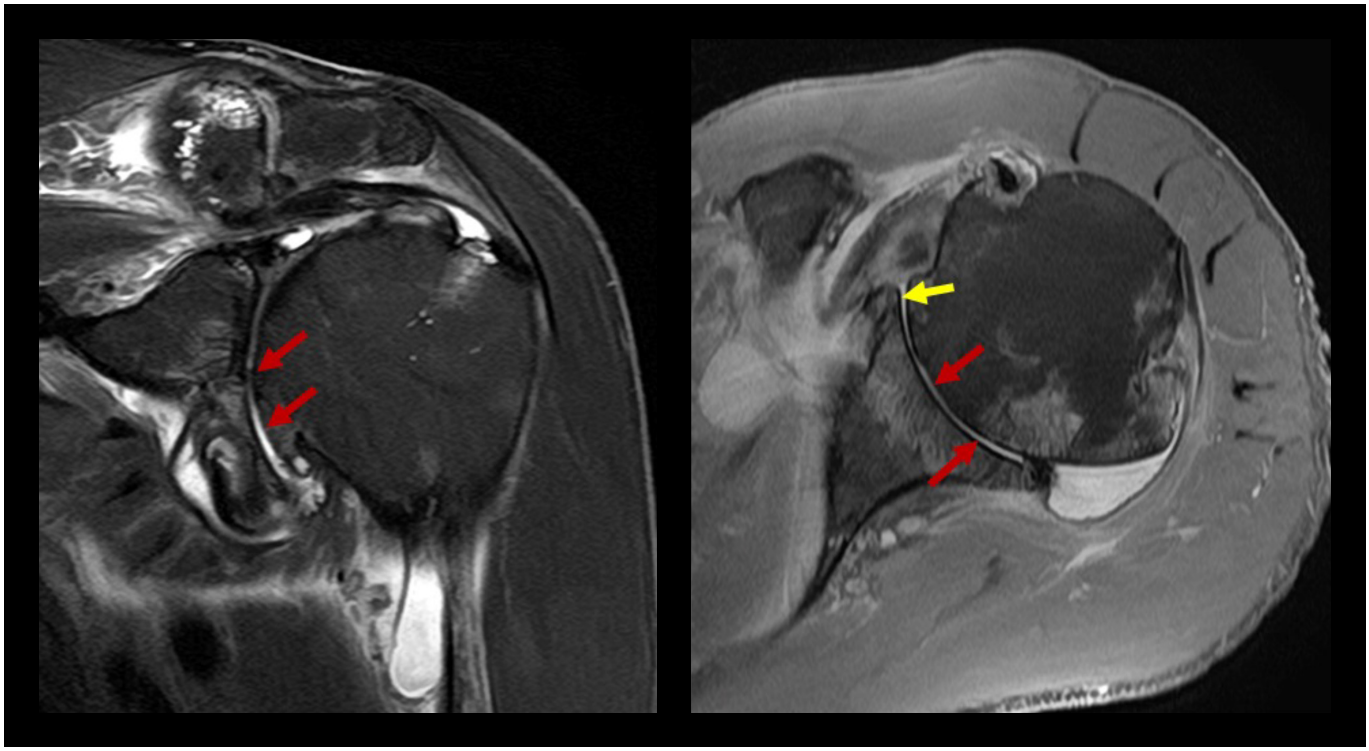

Figure 3.3: AiCE DL reconstructed COR T2 FatSat (left) and AX PD FatSat (right). Yellow arrow shows severe degeneration undermining attenuation and tearing of labrum circumferentially. Red arrows show grade 4 severe chondral thinning to the humeral head and glenoid bone.

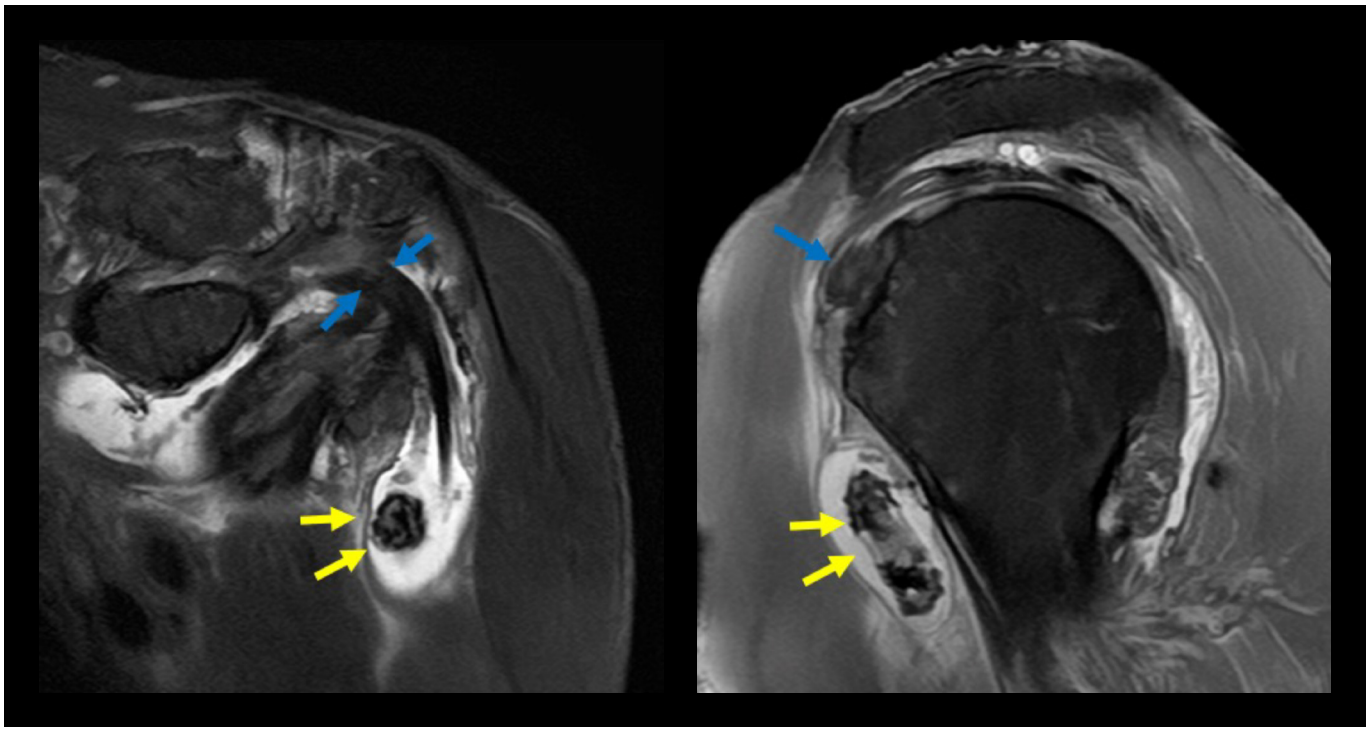

Figure 3.4: AiCE DL reconstructed COR T2 FatSat (left) and SAG PD FatSat (right). Yellow arrows show multiple internal bodies with fluid distension within the bicep tendon sheath. Blue arrows show severe tendinosis with longitudinal fusiform globular thickening hypertrophy of the bicep tendon.

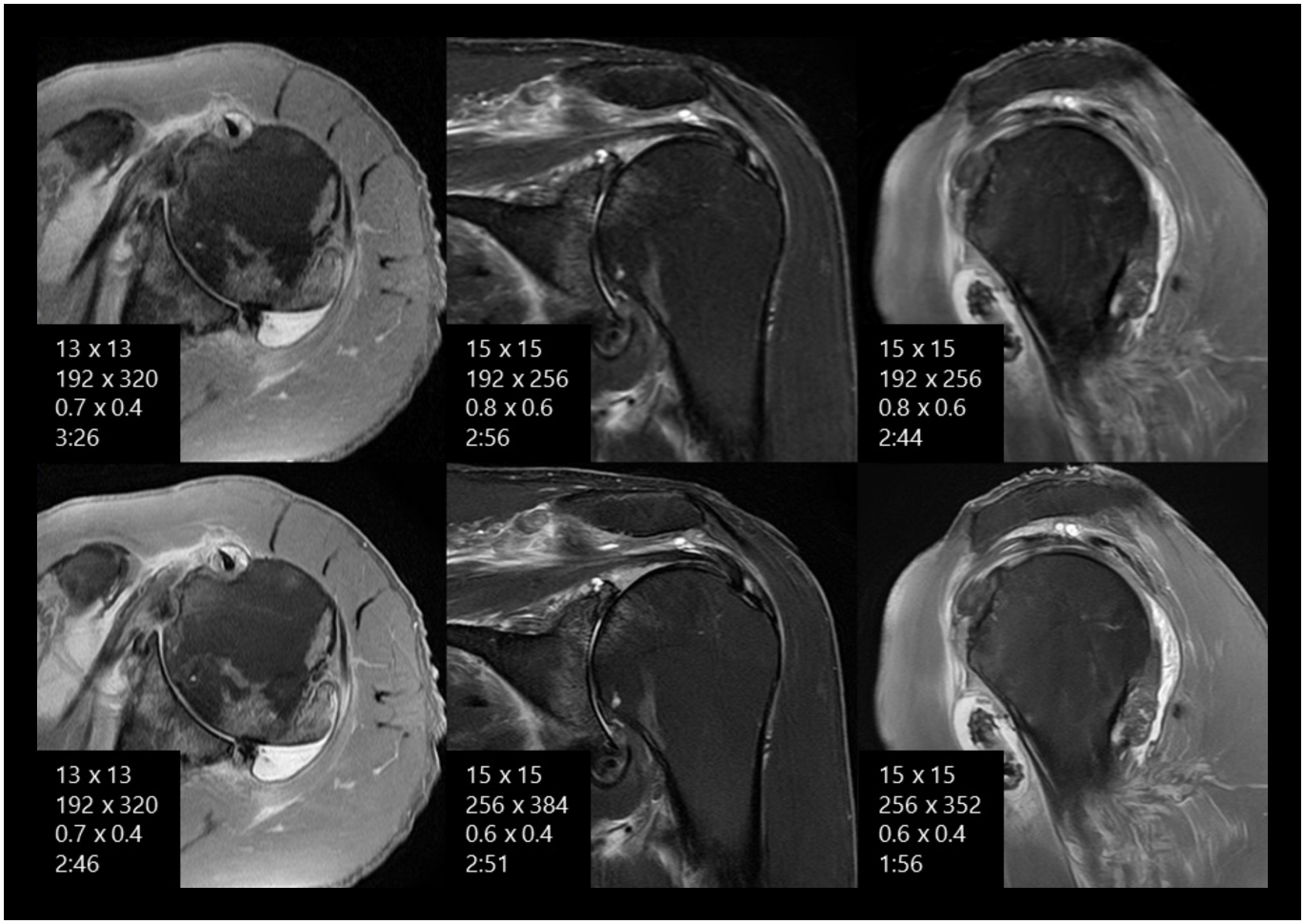

Figure 3.5: Routine images (top row) compared to the AiCE DLR-optimized images (bottom row) with higher resolution and/or shortened scan time.*

Case 3: Shoulder MRI with AiCE DLR						
	AX PD FatSat		COR T2 FatSat		SAG PD FatSat	
	Routine	**AiCE DLR**	**Routine**	**AiCE DLR**	**Routine**	**AiCE DLR**
FOV	13 x 13	13 x 13	15 x 15	15 x 15	15 x 15	15 x 15
Matrix	192 x 320	192 x 320	192 x 256	256 x 384	192 x 256	256 x 352
Resolution (mm^2)	0.68 x 0.41 (0.28)	0.68 x 0.41 (0.28)	0.78 x 0.59 (0.46)	0.59 x 0.39 (0.23)	0.78 x 0.59 (0.46)	0.59 x 0.43 (0.25)
% Resolution Improvement*		**0%**		**50%**		**45.45%**
Scan Time (Seconds)	3:26 (206)	2:46 (166)	2:56 (176)	2:51 (171)	2:44 (164)	1:56 (116)
% Scan Time Reduction*		**19.42%**		**2.84%**		**29.27%**

	Routine	**AiCE DLR**
Total Scan Time (Seconds)	9:06 (546)	7:33 (453)
% Total Scan Time Reduction*		**17.03%**

	Routine	**AiCE DLR**
Average Resolution (mm^2)	0.75 x 0.53 (0.39)	0.62 x 0.41 (0.25)
% Average Resolution Improvement*		**36.02%**

Table 3: Sequence parameters of the routine protocol and the AiCE DLR-optimized protocol.

* Resolution and scan times vary by case. AiCE DLR-optimized protocol scan times and resolution are determined by the operator.

Case #4: Hip MRI with AiCE DLR

MRI of the Left Hip—58-year-old male.

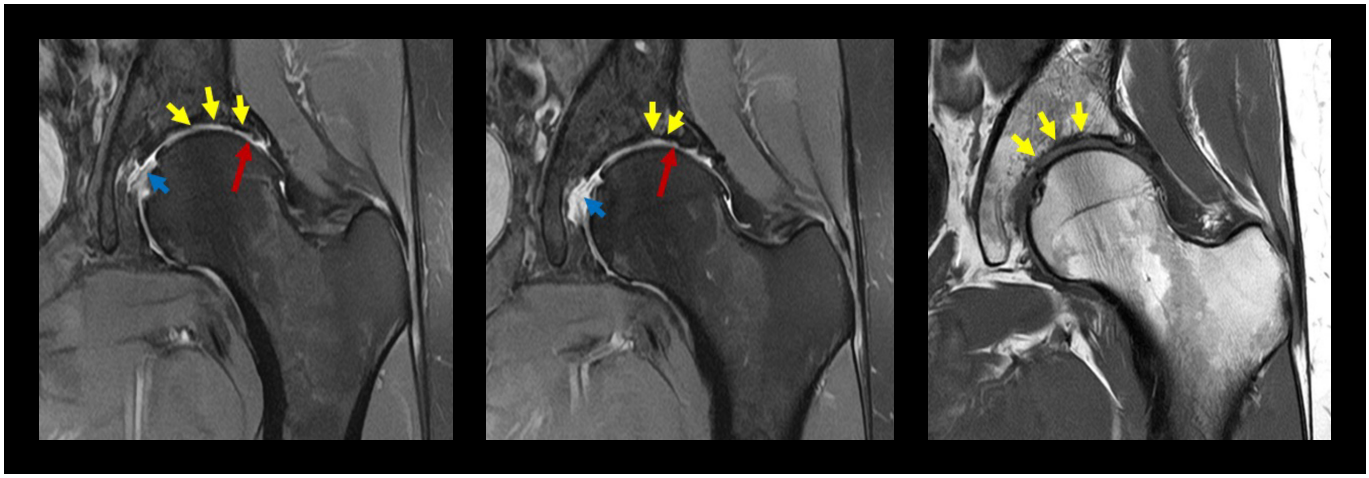

Figure 4.1: AiCE DL reconstructed COR PD FatSat (left and middle) and COR T1 (right). Red arrows show anterior lateral to posterior lateral labral fraying and undermining. Yellow arrows show severe chondral thinning of the anterior lateral to posterior lateral acetabulum and superior lateral femoral head with subchondral bone flattening and irregularity. Blue arrows show irregular tearing and scarring of ligamentum teres.

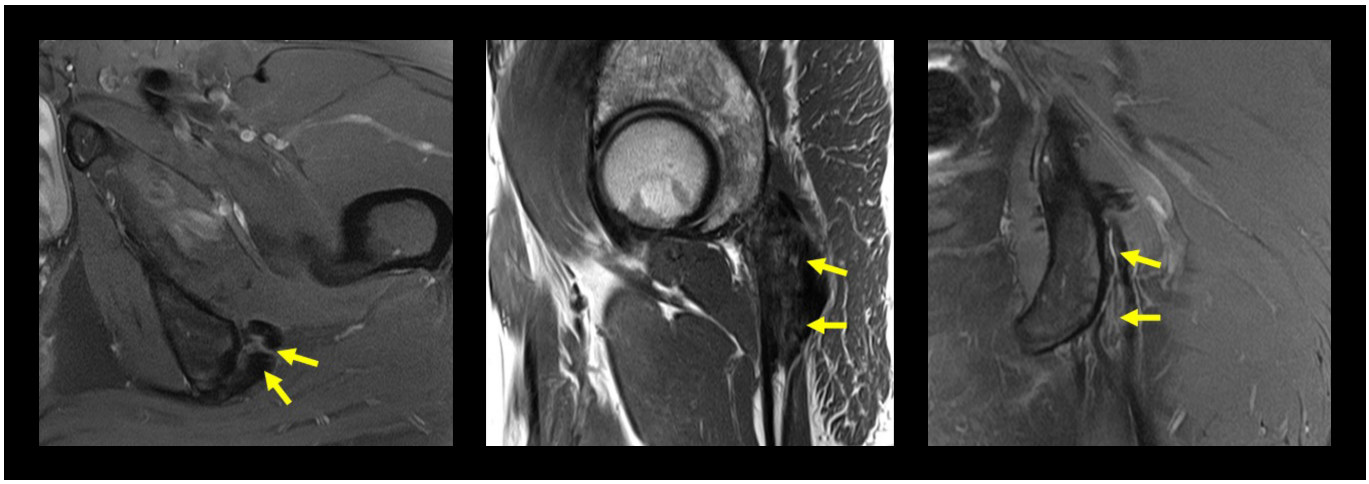

Figure 4.2: AiCE DL reconstructed AX PD FatSat (left), SAG PD (middle), and COR PD FatSat (right). Yellow arrows show proximal left hamstring tendinosis and scarring at ischial tuberosity.

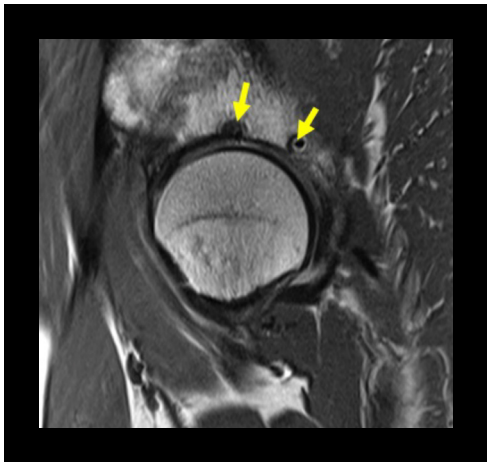

Figure 4.3: AiCE DL reconstructed SAG PD. Yellow arrows demonstrate anterior lateral to posterior lateral labral repair anchors and scarring.

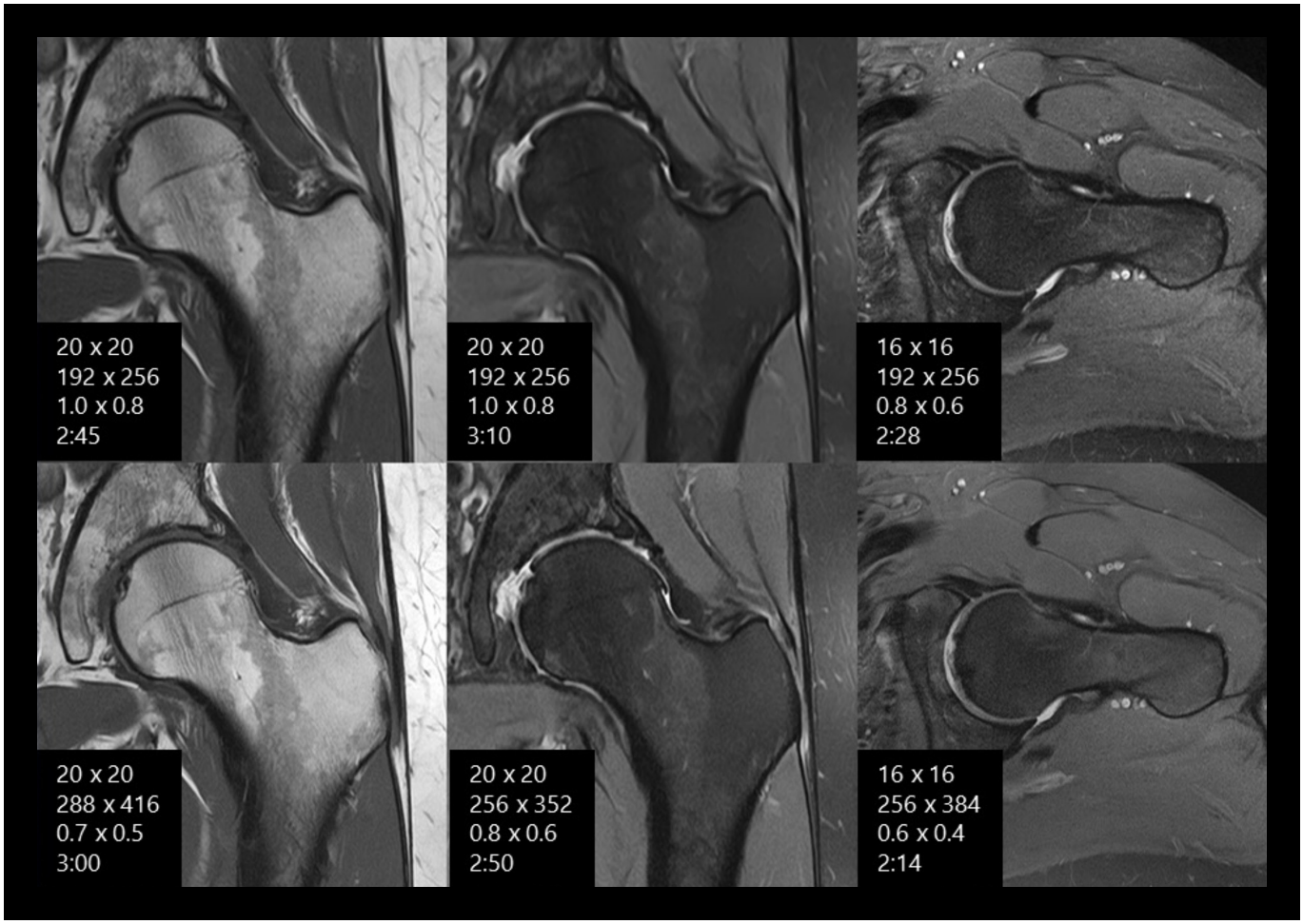

Figure 4.4: Routine images (top row) compared to the AiCE DLR-optimized images (bottom row) with higher resolution and/or shortened scan time.*

Case 4: Hip MRI with AiCE DLR						
	COR T1		COR PD FatSat		AX PD FatSat	
	Routine	**AiCE DLR**	**Routine**	**AiCE DLR**	**Routine**	**AiCE DLR**
FOV	20 x 20	20 x 20	20 x 20	20 x 20	16 x 16	16 x 16
Matrix	192 x 256	288 x 416	192 x 256	256 x 352	192 x 256	256 x 384
Resolution (mm^2)	1.04 x 0.78 (0.81)	0.69 x 0.48 (0.33)	1.04 x 0.78 (0.81)	0.78 x 0.57 (0.44)	0.83 x 0.63 (0.52)	0.63 x 0.42 (0.26)
% Resolution Improvement*		**58.97%**		**45.45%**		**50.00%**
Scan Time (Seconds)	2:45 (165)	3:00 (180)	3:10 (190)	2:50 (170)	2:28 (148)	2:14 (134)
% Scan Time Reduction*		**NA**		**10.53%**		**9.56%**

	Routine	**AiCE DLR**
Total Scan Time (Seconds)	8:23 (503)	8:04 (484)
% Total Scan Time Reduction*		**3.78%**

	Routine	**AiCE DLR**
Average Resolution (mm^2)	0.97 x 0.73 (0.71)	0.70 x 0.49 (0.34)
% Average Resolution Improvement*		**51.74%**

Table 4: Sequence parameters of the routine protocol and the AiCE DLR-optimized protocol.

* Resolution and scan times vary by case. AiCE DLR-optimized protocol scan times and resolution are determined by the operator.

Summary

MRI has established itself to be a powerful imaging modality for noninvasive musculoskeletal system assessment. In MSK MRI, higher SNR and resolution are desired for better delineation of anatomical and pathological features. Conventionally, MRI allows the acquisition of images with higher resolution and SNR; however, with an unavoidable tradeoff of longer scan time. This case study report demonstrates that AiCE DLR removes noise and improves SNR. The SNR improvement may help clinicians in providing flexibility in scan parameters and be used to help alleviate the fundamental tradeoffs between SNR, resolution, and scan time. This case study report demonstrates how AiCE DLR may help the clinicians to increase resolution and/or shorten scan time while allowing preferred image quality.

Canon
CANON MEDICAL SYSTEMS USA, INC
https://us.medical.canon

2441 Michelle Drive, Tustin, CA 92780 | 800.421.1968

MRCS14284US

Made For life